

Non-Rigid Registration of Multiphoton Microscopy Images Using B-Splines

Kevin S. Lorenz^a, Paul Salama^b, Kenneth W. Dunn^c, Edward J. Delp^a

^aVideo and Image Processing
Laboratory
School of Electrical and
Computer Engineering
Purdue University
West Lafayette, Indiana 47907

^bDepartment of Electrical and
Computer Engineering
Indiana University-Purdue University
Indianapolis
Indianapolis, Indiana 46202

^cDivision of Nephrology
School of Medicine
Indiana University
Indianapolis, Indiana 46202

ABSTRACT

Optical microscopy poses many challenges for digital image analysis. One particular challenge includes correction of image artifacts due to respiratory motion from specimens imaged *in vivo*. We describe a non-rigid registration method using B-splines to correct these motion artifacts. Current attempts at non-rigid medical image registration have typically involved only a single pair of images. Extending these techniques to an entire series of images, possibly comprising hundreds of images, is presented in this paper. Our method involves creating a uniform grid of control points across each image in a stack. Each control point is manipulated by optimizing a cost function consisting of two parts: a term to determine image similarity, and a term to evaluate deformation grid smoothness. This process is repeated for all images in the stack. Analysis is evaluated using block motion estimation and other visualization techniques.

Keywords: image registration, b-splines, microscopy

1. INTRODUCTION

Optical microscopy image sets may be obtained from live specimens via a technique known as intravital microscopy. These studies frequently involve collecting a series of images, either for characterizing three-dimensional volumes of the specimen or for studying biological processes in time series. These image volumes are compromised to varying degrees by motion artifacts resulting from factors such as respiration and heartbeat. These factors change the position and shape of the sample volume such that sequential images are not registered with one another. These motion-induced artifacts can be addressed through the use of image registration, which aligns the images (spatially and/or temporally) so that they all share a common coordinate system, a condition aiding in future image analysis. The process is often described as finding an explicit function that performs a backward mapping of a target image onto a source image.^{1,2} It is often desirable to transform information obtained from multiple images into a single common coordinate system encompassing the knowledge available from all the various source images.³

There exists much controversy over approaches to image registration with confocal and multiphoton microscopy. Some argue⁴ that user interaction is best suited since no automated procedure can truly reproduce the accuracy of a human in correctly identifying individual cellular objects. While the entire process is not completely manual, it requires at least a manual input of an initial seed value or starting point. Additionally, several authors have based their registration schemes on manually selecting landmarks.⁵⁻⁷ However, this quickly becomes impractical as the number of images in a stack approaches hundreds of images. Therefore, others argue⁸ that a completely automated process is necessary to obtain quantitative, objective, and repeatable results. User interaction causes varying results for identical input data sets which may be unacceptable in certain applications. Nonetheless, automatic image registration is absolutely necessary for quantification of multiphoton image volumes, whose size and complexity makes manual image registration impractical. Additionally, current registration methods, when applied to medical imaging, are typically very sensitive to small changes in parameters, causing inconsistent and unpredictable results.⁹

The general goal of our work is to register a sequence or “stack” of multiphoton fluorescence microscopy images. This paper describes a non-rigid registration technique using B-splines we have developed for such

images. A typical data set we analyze for registration may consist of approximately one hundred images of renal or liver tissue acquired *in vivo* from a rat. The images are acquired sequentially either from a single focal plane in the specimen at evenly spaced time intervals (time-series data) or from a series of evenly spaced focal planes (three-dimensional data). Additionally, each image consists of three different channels, corresponding to the fluorescence of three different probes introduced into the rat, collected simultaneously by three different photomultiplier detectors. When viewing these multi-channel data sets, the colors displayed are not due to the biological structures truly being the color shown, but because of the color palette used in assigning color to each of the three channels of the multiphoton microscope.

Intravital microscopy is a powerful technique for studying physiological processes in the most relevant context, in the living animal. However, developing assays of physiological function will require developing novel methods of digital image analysis that will support quantitative analysis. Insofar as accurate image registration is prerequisite to quantitative analysis of time series and volumetric image data, the development of effective methods of image registration is fundamentally important to realizing the potential of intravital microscopy as a tool for understanding and treating human diseases.

Multiphoton microscopy image stacks contain many unique characteristics that make analysis challenging. Objects contained within time-series data sets typically have poorly defined edges. Object boundaries are not composed of rigid continuous edges. Instead, noise, low image resolution, and the dynamic nature of biological tissues contribute to creating sparse edges along with irregular and inconsistent patterns within objects. Tissue is not homogeneous, and traditional registration techniques, including edge detection and landmark based methods, have given poor results.

2. METHOD

Image registration is the task of finding a function mapping coordinates from a moving test image to corresponding coordinates in a reference image. In this paper, we describe a non-rigid registration method we have developed to address the motion artifacts and non-linear distortions caused by respiration and heartbeat evident in microscopy images. In particular, we will investigate a non-rigid registration technique using B-splines, which also allows for easy visualization of the distortion and leads to a realistically registered image. This method, which is an extension of the work proposed by Rueckert et al.,¹⁰ deforms an image by first establishing an underlying mesh of control points, and then manipulates these control points in a manner that maintains a smooth and continuous transformation. To begin, a grid of control points, $\phi_{i,j}$, is initially constructed with equal spacings δ_x and δ_y between points, in the horizontal and vertical directions, respectively. The non-rigid transformation \mathbf{T} of a point (x, y) in the moving image to the corresponding point (x', y') in the reference image is given by the mapping $\mathbf{T}(x, y) \rightarrow (x', y')$.¹¹

$$\mathbf{T}(x, y) = \sum_{l=0}^3 \sum_{m=0}^3 B_l(u) B_m(v) \phi_{i+l, j+m} \quad (1)$$

where $i = \lfloor x/\delta_x \rfloor - 1$ and $j = \lfloor y/\delta_y \rfloor - 1$ are the indices of the nearest control point $\phi_{i,j}$ to the above and to the left of (x, y) , and $u = x/\delta_x - \lfloor x/\delta_x \rfloor$ and $v = y/\delta_y - \lfloor y/\delta_y \rfloor$ are such that (u, v) is the relative position of (x, y) relative to $\phi_{i,j}$. Additionally, B_l represents the l -th basis function of the B-spline.¹²

$$\begin{aligned} B_0(t) &= (1-t)^3/6 \\ B_1(t) &= (3t^3 - 6t^2 + 4)/6 \\ B_2(t) &= (-3t^3 + 3t^2 + 3t + 1)/6 \\ B_3(t) &= t^3/6 \end{aligned} \quad (2)$$

As previously stated, in addition to the non-rigid deformation maximizing the similarity between the registered image and the reference image, the deformation must also be realistic and smooth. To constrain the deformation field to be smooth, a penalty term to regularize the transformation is introduced as:^{13,14}

$$C_{smooth} = \frac{1}{A} \int_0^X \int_0^Y \left[\left(\frac{\partial^2 \mathbf{T}}{\partial x^2} \right)^2 + \left(\frac{\partial^2 \mathbf{T}}{\partial y^2} \right)^2 + 2 \left(\frac{\partial^2 \mathbf{T}}{\partial x \partial y} \right)^2 \right] dx dy \quad (3)$$

This regularization is necessary because each pixel in the image is free to move independently. As such, it is possible that all pixels with one particular intensity in the moving image map to a single pixel having this same intensity in the reference image, and the resulting deformation field will be unrealistic.¹⁵ This is one of the primary reasons why non-rigid image registration is considered difficult, as an appropriate balance and compromise must be reached between allowing large amounts of independent movement and smoothness of the transformation.

The optimal deformation of the grid of control points is found by optimizing a cost function. This cost function includes two terms with two competing goals. The first goal is to maximize the similarity and alignment between the reference image and the deformed moving or registered image. The second goal is to smooth and regularize the deformation to create a realistic transformation. This cost function is written as:

$$C_{total} = C_{similarity}(I_{reference}(x, y), I_{moving}(\mathbf{T}(x, y))) + \lambda C_{smooth}(\mathbf{T}) \quad (4)$$

where λ is a weighting coefficient which defines the tradeoff between the two competing cost terms. The similarity metric, $C_{similarity}$, may be defined as one of numerous possibilities, including sum of squared differences, sum of absolute differences, or normalized mutual information, whichever may fit the particular image set best. In our work, we have chosen $C_{similarity}$ to have decreasing value for increasingly similar images (i.e. two identical images have $C_{similarity} = 0$). With such an approach, and by also wanting to minimize sharp warping elements of the transformation \mathbf{T} defined in C_{smooth} , we desire to minimize C_{total} as well.

The resolution of the grid of control points affects the degree of deformation allowed, and hence affects how readily $C_{similarity}$ may be minimized. A large, sparse spacing of control points corresponds with a more global non-rigid deformation, which may not allow $C_{similarity}$ to reach values near zero. Alternatively, a small, dense spacing of control points corresponds with highly local non-rigid deformations and more readily allows $C_{similarity}$ to reach values near zero. In our work, we have experimented with various grid spacing values, and have found that values that work well are highly dependent on image size, the content of these images, and the degree of motion artifacts present throughout the stack of images.

In addition, this non-rigid registration method assumes grayscale, single channel images, not multi-channel (multiple component) images. Therefore, a particular channel must be selected to perform registration on. Directly using one of the multiple channels for registration may be the quick and logical choice. However, there are many regions in each image where a particular channel exhibits/contributes very little signal. As a result, these regions are registered improperly. Therefore, perhaps contrary to logical assumption, a composite gray level channel created from the luminance component of the image is an appropriate image to use with this registration method. Even though a linear combination of the three channels has no biological significance, using gray level composite images for registration corrected significantly more motion artifacts than using any other channel. In this work, we construct this gray level image by computing the luminance component of the image:

$$x_{gray} = 0.2989 * x_{red} + 0.5870 * x_{green} + 0.1140 * x_{blue} \quad (5)$$

where x_{red} , x_{green} , and x_{blue} denote the red, green, and blue components of the input image x , respectively.

Finally, for each image, a final deformation field based on the gray level image was obtained. This deformation field was then used to transform all channels of the image. In order to register an entire stack of images, the moving test image was chosen to be the current image, and the reference image was chosen to be the previously registered image. Therefore, the cost function is more precisely defined as:

$$C_{total} = C_{similarity}(I'_{n-1}(x, y), I_n(\mathbf{T}(x, y))) + \lambda C_{smooth}(\mathbf{T}) \quad (6)$$

where n denotes the image number and I' denotes a registered image.

3. EXPERIMENTAL RESULTS

We now introduce an example three-channel data set containing severe non-linear motion artifacts. We have depicted the results from a sequence of three consecutive images from this data set to demonstrate our non-rigid registration method. By progressing from one image to the next, significant motion artifacts are visible as horizontally banded regions of the scene are warped to the upper-left. In the subsequent image, the objects are restored to their unwarped original locations. In a scanning multiphoton fluorescence microscope, the two-dimensional image is assembled by sequentially scanning a series of horizontal lines across a sample. Because of the method of scanning, adjacent pixels are collected only microseconds apart in the horizontal direction, but are collected milliseconds apart in the vertical direction. For this reason, motion artifacts frequently appear in horizontal banding patterns.

Figure 1 shows the results from B-spline registration along with the deformation grid corresponding to the warping of the moving image to the reference image. These results were obtained by performing registration using $\lambda = 0.01$ and a B-spline control point grid spacing of $\delta_x = \delta_y = 64$ pixels, and using a limited memory Broyden-Fletcher-Goldfarb-Shanno (LBFGS) optimizer to determine the final B-spline control points. Our similarity metric, $C_{similarity}$, was defined as mean squared error:

$$C_{similarity}(I_x, I_y) = \frac{1}{M * N} \sum_{m=0}^{M-1} \sum_{n=0}^{N-1} (I_x(m, n) - I_y(m, n))^2 \quad (7)$$

where M and N denote the height and width of the image in pixels, respectively.

A common issue with intravital microscopy is the lack of ground truth data due to limitations of image acquisition equipment and ethical concerns. Therefore, evaluating the accuracy of results proves challenging. Although block motion estimation does not lend itself well to image registration directly, we will use this method in an attempt to objectively gauge the performance of our non-rigid B-spline registration method. Block motion estimation is an integral component of video coding and compression, and has the strong ability to identify localized motion patterns from one image to the next. A consequence of dividing the image into equally sized blocks is that it does not provide an easy and obvious way to correct these motions and produce a viable and realistically registered image. Traditionally, following block motion estimation, a motion compensated image is created by displacing each block in the image by its associated motion vector. This may increase the similarity between the motion compensated image and the original image according to some defined cost metric. However, the motion compensated image has obvious block artifacts, creating an unrealistic image. However, since block motion estimation allows for easy visualization, we can objectively compare the quantity and angle of motion vectors before and after non-rigid registration.

The overall idea is that block motion estimation will provide localized information about direction and magnitude of motion throughout each image in a data set. The method for block motion estimation is well-known¹⁶ and proceeds as follows: The current image is divided into a matrix of equally sized blocks of pixels. Each block is then compared with its corresponding equally sized block and its adjacent neighbors in the previous image. The block in the previous image that is most similar to the block in the current image creates a motion vector that predicts the movement of this block from one location in the previous image to its new location in the current image. A motion vector is computed for each block in the matrix for the entire image. The search area of adjacent neighboring blocks in the previous image is constrained to p pixels in all four directions, and will create a $2p + 1 \times 2p + 1$ search window. A larger p is necessary to correctly predict larger motion, but at the same time, this also increases computational complexity.

We specify a 31×31 search window and a 4×4 block size. We maximize similarity between two blocks by minimizing mean squared error (MSE) as our chosen cost function:

$$MSE = \frac{1}{N^2} \sum_{i=0}^{N-1} \sum_{j=0}^{N-1} (C_{ij} - R_{ij})^2 \quad (8)$$

where $N = 4$ is our chosen block size, and C_{ij} and R_{ij} are the pixels being compared in the current and reference blocks, respectively. Several methods have been developed to reduce the computational complexity of this motion

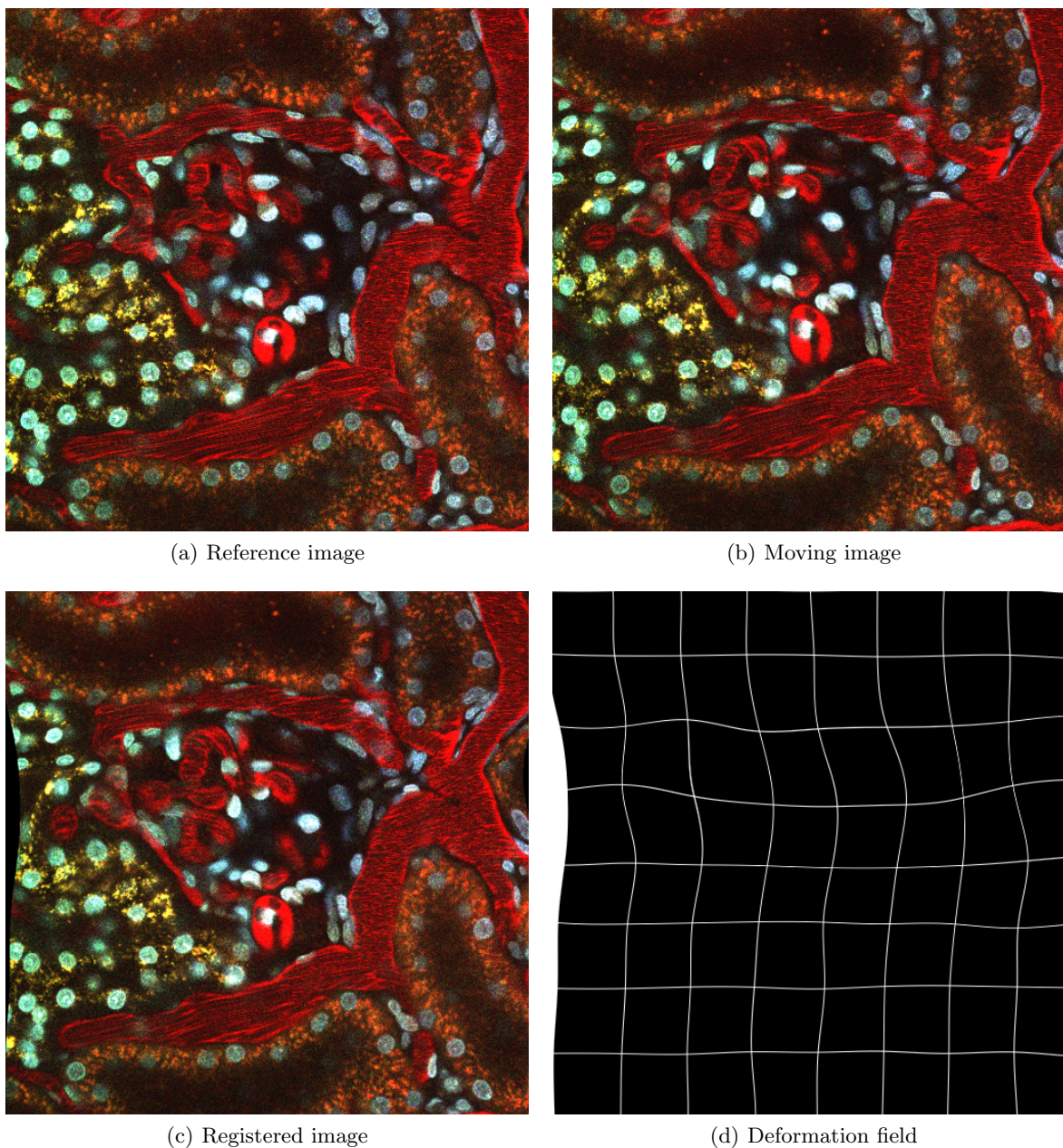


Figure 1. Registration results from example data set.

estimation process. However, we are currently more concerned with accuracy and correctness of our results rather than computational complexity. Therefore, we only utilize the exhaustive search, or full search, method. This method computes the cost function for every block in the search window, requiring $(2p + 1)^2$ comparisons with blocks having N^2 pixels. Thus, it also finds the best possible match.

Computing histograms of angles for motion vectors with non-zero magnitudes attempts to identify any distinct motion patterns within the motion vector field. These histograms, corresponding with the unregistered images, are created with 36 bins. Furthermore, these histograms of motion vector angles are weighted by motion vector magnitude, and are shown in Figure 2. As can be seen, the first image (whose histogram is shown in Figure 2(a)) has a distinct motion to the upper-left, while the next image (whose histogram is shown in Figure 2(b)) has a distinct motion to the lower-right. Likewise, weighted histograms for motion vectors associated with the two

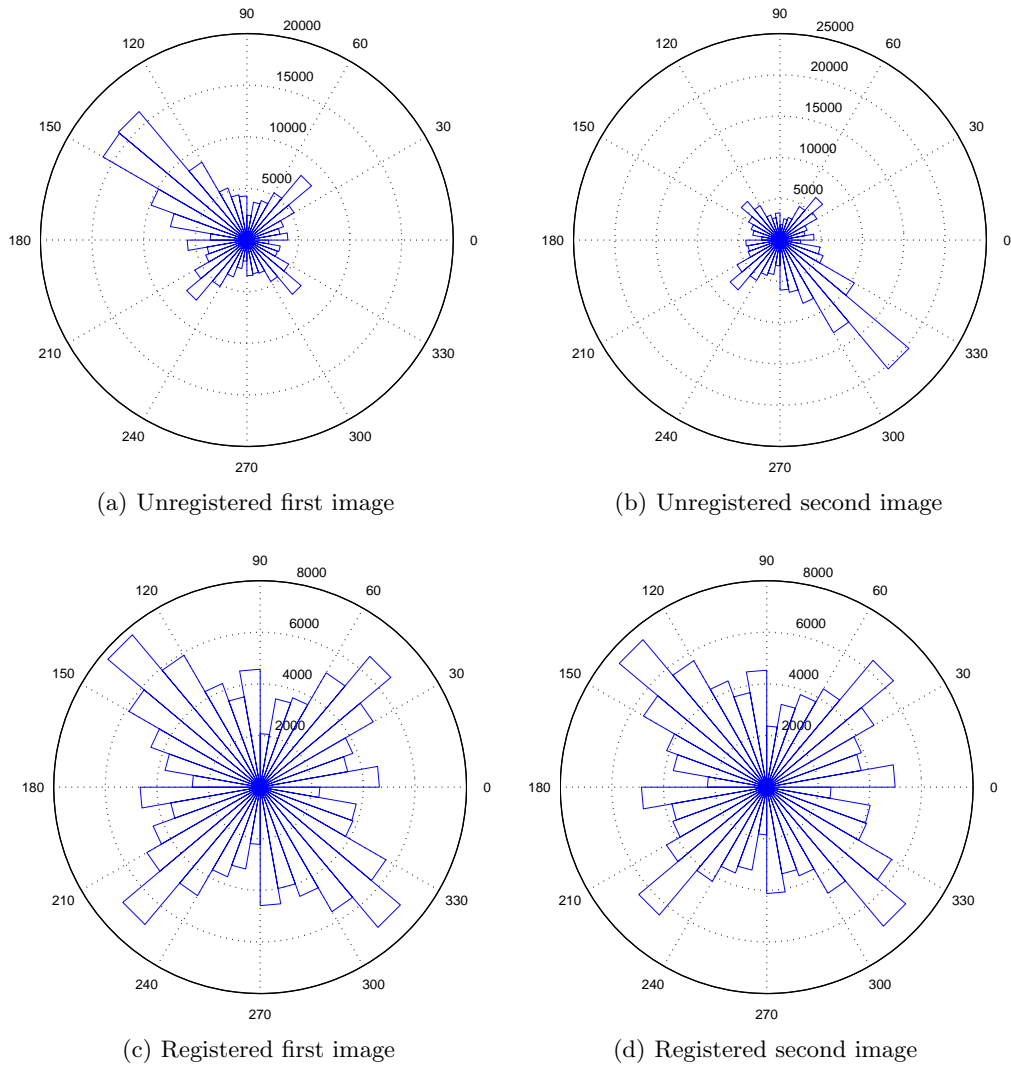
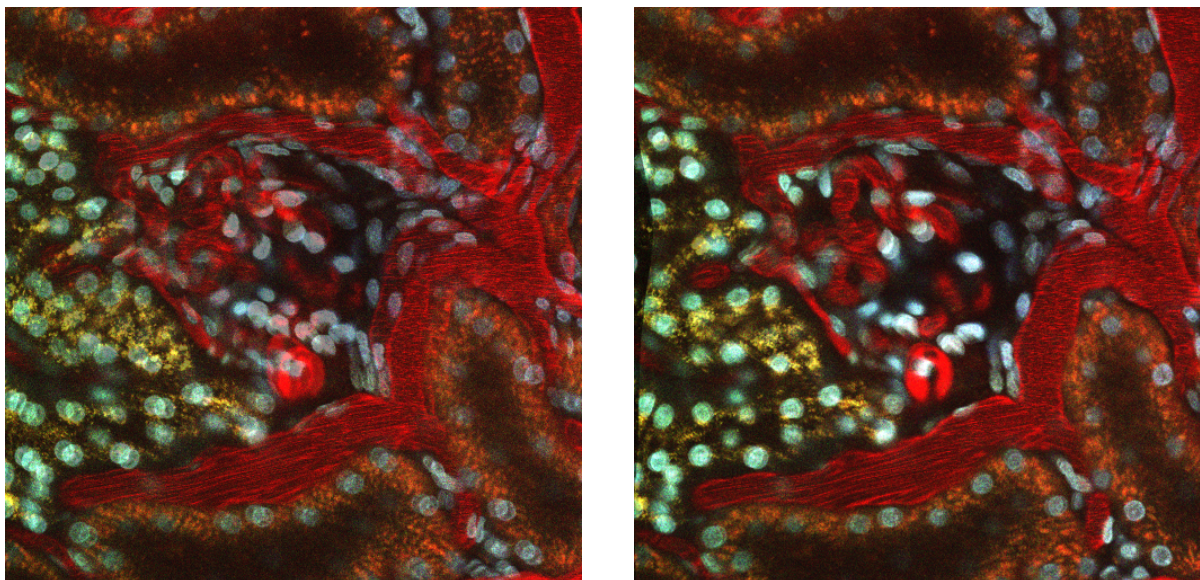


Figure 2. Weighted histograms of motion vector angles.

corresponding registered images are shown in Figure 2(c)-(d), respectively. As can be seen, the distribution of motion vector angles is significantly more uniform for the registered images compared to the unregistered images. This simple comparison indicates that the non-rigid B-spline registration technique has successfully corrected a large portion of the respiratory motion artifacts.

A subjective evaluation of the registration results is performed by overlaying consecutive unregistered images, and comparing this composite overlay image with that for the corresponding consecutive registered images. This comparison is shown in Figure 3. Ghosting artifacts are easily visible in the unregistered overlay image, due to significant misalignment of objects. However, this ghosting is vastly reduced in the registered overlay image. Therefore, this visual inspection of the registration results confirms that the motion artifacts have largely been corrected.

As an additional way to evaluate our non-rigid registration results, we compared these results to those from another method known as Thirion's "demons" algorithm.^{17,18} This technique is an iterative non-rigid registration method that borrows concepts from optical flow. The results using demons algorithm for the same representative image are shown in Figure 4. As can be seen, these results need significant improvement. From visual inspection, the motion artifacts within the vascular structures in the red channel are exaggerated rather than corrected. In the blue channel, nuclei are no longer round as expected. Instead, nuclei become oblong and transform into



(a) Unregistered images

(b) Registered images

Figure 3. Overlay of consecutive images from example data set.

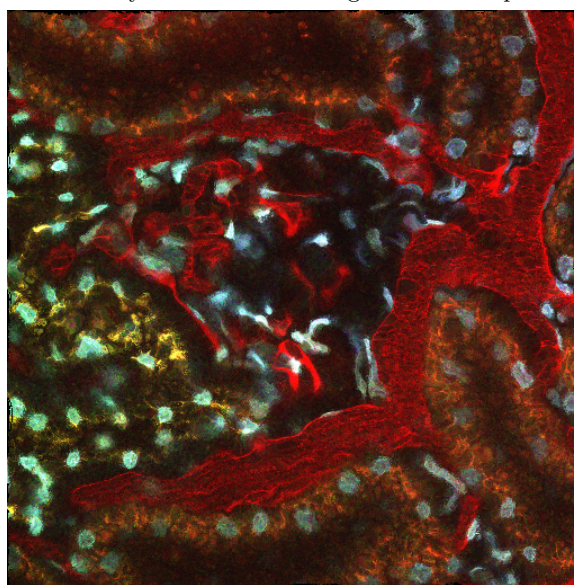


Figure 4. Registration results from demons algorithm.

other irregular shapes. These issues persisted across all images registered in the stack. Therefore, we conclude that non-rigid B-spline registration improves upon demons algorithm for multiphoton microscopy images.

4. CONCLUSIONS

This paper described an automatic method to non-rigidly register a stack or series of multiphoton intravital microscopy images. User interaction may be introduced to modify certain parameters of the analysis, including control point grid spacing and the similarity cost coefficient. Experimental results indicated that this method is promising in correcting minor to moderate image artifacts due to respiration, heartbeat, and other specimen motion. Objective evaluation of our results proves to be difficult due to the lack of ground truth data. Evaluation of results has been initially addressed through the use of block motion estimation, and also through visual inspection of overlaying of unregistered and registered images.

ACKNOWLEDGMENTS

This work was supported by the National Institutes of Health (NIH) under Grant P30 DK079312-03 (KD). Data was collected by Ruben Sandoval at the Indiana Center for Biological Microscopy.

REFERENCES

- [1] Brown, L., "A survey of image registration techniques," *ACM Computing Surveys* **24**(4), 325–376 (1992).
- [2] Zitová, B. and Flusser, J., "Image registration methods: A survey," *Image and Vision Computing* **21**, 977–1000 (October 2003).
- [3] Hajnal, J., Hill, D., and Hawkes, D., [*Medical Image Registration*], CRC Press (2001).
- [4] McCullough, D., Gudla, P., Harris, B., Collins, J., Meaburn, K., Nakaya, M.-A., Yamaguchi, T., Misteli, T., and Lockett, S., "Segmentation of whole cells and cell nuclei from 3-D optical microscope images using dynamic programming," *IEEE Transactions on Medical Imaging* **27**, 723–734 (May 2008).
- [5] Bazen, A. and Gerez, S., "Fingerprint matching by thin-plate spline modeling of elastic deformations," *Pattern Recognition* **36**(8), 1859–1867 (2003).
- [6] Rohr, K., Stiehl, H., Sprengel, R., Buzug, T., Weese, J., and Kuhn, M., "Landmark-based elastic registration using approximating thin-plate splines," *IEEE Transactions on Medical Imaging* **20**, 526–534 (June 2001).
- [7] Pánek, J. and Vohradský, J., "Point pattern matching in the analysis of two-dimensional gel electropherograms," *Electrophoresis* **20**(18), 3483–3491 (1999).
- [8] Luck, B., Carlson, K., Bovik, A., and Richards-Kortum, R., "An image model and segmentation algorithm for reflectance confocal images of in vivo cervical tissue," *IEEE Transactions on Image Processing* **14**, 1265–1276 (September 2005).
- [9] Kyan, M., Guan, L., Arnison, M., and Cogswell, C., "Feature extraction of chromosomes from 3-D confocal microscope images," *IEEE Transactions on Biomedical Engineering* **48**, 1306–1318 (November 2001).
- [10] Rueckert, D., Sonoda, L., Hayes, C., Hill, D., Leach, M., and Hawkes, D., "Nonrigid registration using free-form deformations: application to breast MR images," *IEEE Transactions on Medical Imaging* **18**, 712–721 (August 1999).
- [11] Mazaheri, Y., Bokacheva, L., Kroon, D.-J., Akin, O., Hricak, H., Chamudot, D., Fine, S., and Koutcher, J. A., "Semi-automatic deformable registration of prostate MR images to pathological slices," *Journal of Magnetic Resonance Imaging* **32**, 1149–1157 (April 2010).
- [12] Lee, S., Wolberg, G., and Shin, S., "Scattered data interpolation with multilevel b-splines," *IEEE Transactions on Visualization and Computer Graphics* **3**, 228–244 (July-September 1997).
- [13] Sorzano, C., Thévenaz, P., and Unser, M., "Elastic registration of biological images using vector-spline regularization," *IEEE Transactions on Biomedical Engineering* **52**, 652–663 (April 2005).
- [14] Rohlfing, T., Maurer Jr., C., Bluemke, D., and Jacobs, M., "Volume-preserving nonrigid registration of MR breast images using free-form deformation with an incompressibility constraint," *IEEE Transactions on Medical Imaging* **22**, 730–741 (June 2003).
- [15] Pennec, X., Cachier, P., and Ayache, N., "Understanding the "demon's algorithm": 3D non-rigid registration by gradient descent," *Proceedings of the Second International Conference on Medical Image Computing and Computer-Assisted Intervention*, 597–605 (1999).
- [16] Jain, J. and Jain, A., "Displacement measurement and its application in interframe image coding," *IEEE Transactions on Communications* **29**, 1799–1808 (December 1981).
- [17] Thirion, J.-P., "Non-rigid matching using demons," *Proceedings of the IEEE Computer Society Conference on Computer Vision and Pattern Recognition*, 245–251 (June 1996).
- [18] Thirion, J.-P., "Image matching as a diffusion process: an analogy with maxwell's demons," *Medical Image Analysis* **2**(3), 243–260 (1998).